

## Effect of properties of SiC fibers on longitudinal tensile behavior of SiC<sub>f</sub>/Ti-6Al-4V composites

LI Jian-kang(李建康), YANG Yan-qing(杨延清), YUAN Mei-ni(原梅妮),  
LUO Xian(罗 贤), LI Li-li(李丽丽)

School of Materials Science and Engineering, Northwestern Polytechnical University, Xi'an 710072, China

Received 31 July 2007; accepted 7 December 2007

**Abstract:** Three types of SiC fibers with different tensile strength were employed to prepare unidirectional titanium matrix composites. The strengths of the original SiC fibers and extracted fibers from the composites were measured. The results show that the mechanical properties of fibers are greatly damaged by the consolidation processing of the composite. The strength data of the extracted fibers are used to predict the strength of the composites according to two theoretic models. The Globe Load-Sharing(GLS) model overestimates the strength of the composites. If the Local Load-Sharing(LLS) model assumes that failure occurs after the formation of a cluster with three broken fibers, the model can predict the strength of the composites exactly.

**Key words:** SiC fiber; titanium-matrix composites; Weibull distribution; tensile strength

### 1 Introduction

SiC fiber reinforced titanium metal matrix composites(TMCs) are being developed for application in future aeronautical gas-turbine engines because of their improved mechanical properties compared with monolithic titanium alloys. TMCs exhibit superior mechanical properties along the fiber direction, such as tensile strength, stiffness, creep resistance, and fatigue crack growth resistance at room and elevated temperatures[1–8]. Although the TMCs' mechanical behavior can be depicted by the Rule of Mixtures in terms of the thermal residual stresses, it is very complicated to calculate the longitudinal tensile strength of TMCs because of the dispersed strength distribution of the reinforcement fibers in nature and the multi-factors to influence the failure tensile strength of TMCs[6–17], such as the interfacial structure and mechanical properties, the residual stress and the matrix properties. In the process of loading, some weak fibers will be broken first and the load must be transferred to other unbroken fibers. There are two models to describe the load transferring[7–8]. The first is so-called Global Load Sharing(GLS) model applying to the composites

with weak interface between fibers and matrix. The model assumes that the load is transferred homogeneously to the other fibers at the same section. Another is Local Load Sharing(LLS) model adapting for the composite with strong interface. The model considers that the loading only transfer to neighbor fibers near a broken one and stress concentration is formed thereafter. Obviously, the strength distribution and surface structure of SiC fibers will influence the properties of TMCs to a great extent.

In this work, three types of SiC fibers with different tensile strength and surface conditions are adopted to prepare TMCs by foil/fiber lay-up technique. The strengths of original fiber and the post-process fiber etched from TMCs are measured and the results are employed to calculate the fracture tensile strength of TMCs using GLS model and LLS model, respectively. The longitudinal tensile strength of three kinds of TMCs is tested in order to compare with the prediction of GLS and LLS models, respectively.

### 2 Experimental

Three types of SiC fibers produced by chemical vapor deposition(CVD) were employed to prepare

TMCs. One named SCS-6 (produced by Textron Systems, Lowell, MA, USA) is carbon-cored, with a diameter of 140  $\mu\text{m}$  and a 3  $\mu\text{m}$ -thick carbon coating on the outer surface[10]. The other two are both homemade and tungsten-cored, with 110  $\mu\text{m}$  in diameter. The only difference of the two is one has no carbon coating (named as No.1 fiber hereafter), and the other has a carbon coating of 2  $\mu\text{m}$  in thickness (No.2 fiber). The thickness of the Ti-6Al-4V alloy foil is 100  $\mu\text{m}$ .

TMCs panels were fabricated through foil/fiber/foil consolidation process. The stacked materials were hot pressed under a pressure of 50 MPa at 910  $^{\circ}\text{C}$  for 40 min. A representative cross-sections of the three types of composite panels are shown in Fig.1, and the thickness of the panels is about 1.2 mm. The composites was fully

densified, and no pores can be detected. The micrographs also reveal that the fibers in the composites are nearly homogeneously arrayed. The fiber volume fractions for all the composites are about 30%.

The dog-bone specimens of 20 mm in gage length and 6 mm in width with the fibers oriented in the loading direction were machined by computer controlled electro-discharge machining. The thickness of the specimens was just that of the as-prepared composite panels. Tensile tests were carried out in a servo-hydraulic testing machine under controlling at an average strain rate of 1 mm/min. Three specimens for each TMCs were measured for the tensile strength measurement.

The in situ mechanical properties of the fibers were obtained from the monofilaments extracted from the composite panel by removing the matrix with an aqueous solution of HF acid of 40%. The extracted fibers were rinsed in water and dried in air at 50  $^{\circ}\text{C}$ .

The strength and its statistical distribution of the SiC fiber were determined through tensile tests in an electronical control tensile machine with full load of about 500 N. The specimen of about 50 mm length was stucked to soft plastic panels at two ends with epoxies. After epoxies consolidating for 8 h, the specimen was carefully clipped on the clamps of the test machine. There was 20 mm distance equal to the gauge length of the specimen between the two heads of clamps. Fifty fibers were measured for each group including original fibers and extracted fibers. All the tests were conducted using 20 mm gauge length with crosshead speed of 1 mm/min.

### 3 Results and discussion

#### 3.1 Tensile properties of extracted SiC fibers and original SiC fibers

The statistical distribution of the fiber strength is generally characterized by the Weibull function as follows[7-8,11]:

$$F(\sigma) = 1 - \exp \left\{ - \left( \frac{\sigma}{\sigma_0} \right)^m \right\} \quad (1)$$

where  $F(\sigma)$  is the cumulative failure probability,  $\sigma$  is the tensile fracture strength of fibers,  $\sigma_0$  is the characteristic strength of the fiber,  $m$  is Weibull modulus (shape parameter) for the fiber strength distribution. The values of  $m$  and  $\sigma_0$  can be determined from the slop and the intercept of the curve of  $\ln[\ln(1/(1-F))]$  vs  $\ln \sigma$ .

Fig.2 shows the effect of consolidation on the mechanical properties of the three types of SiC fibers. After consolidation, the Weibull modulus  $m$  and the characteristic strength of all the fiber are decreased distinctly.

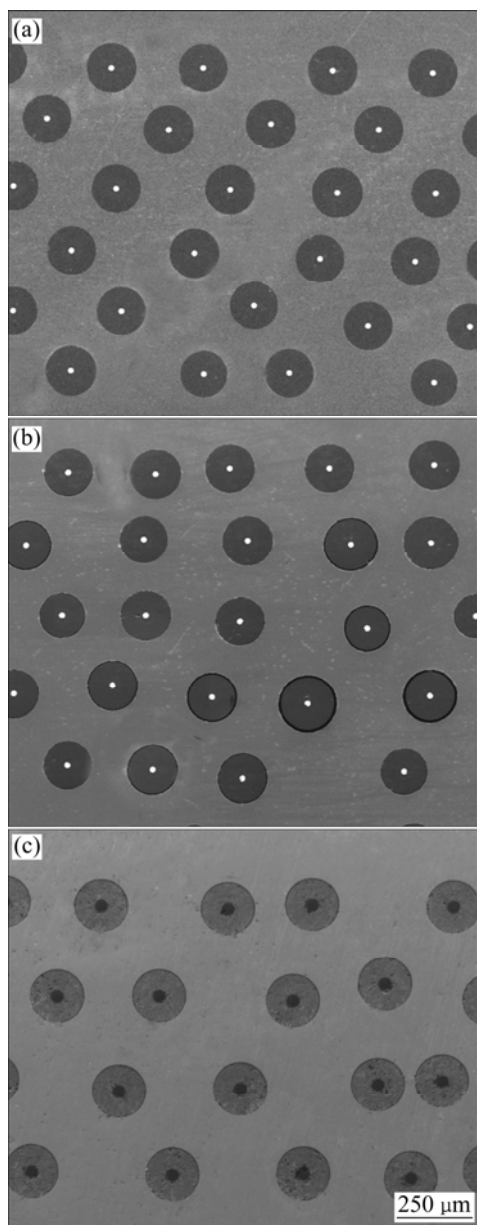


**Fig.1** SEM micrographs of transverse sections of TMCs reinforced by: (a) No.1 fibers; (b) No.2 fibers; (c) SCS-6 fibers

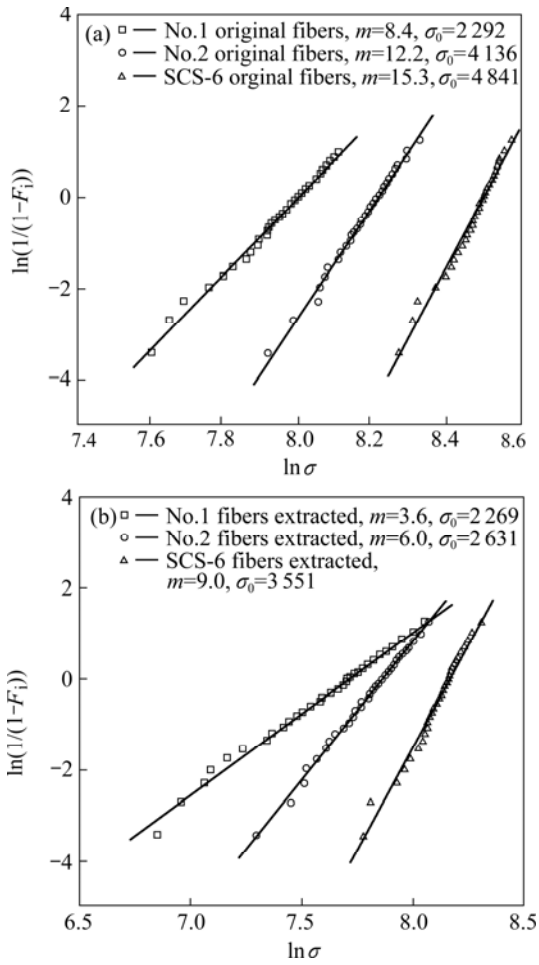


Fig.2 Weibull plots of original (a) and extracted (b) fibers

The surfaces of the three types of SiC fibers in the original and extracted conditions are shown in Fig.3. There is no distinct difference on the surfaces of the original fibers, as shown in Figs.3(a), (b) and (c). Without carbon coating on the surface, No.1 fiber reacts strongly with the matrix titanium alloy, and the surfaces of the fiber are damaged greatly, as shown in Fig.3(d). The extracted No.2 fibers are coated with a thin reaction products and there are no acute defects on the surface, as shown in Fig.3(e). The reaction layer on SCS-6 fiber is broken off easily. Underneath the layer, the surface of the fiber is smooth and there are no reaction erosion defects. So the carbon coating gives benefit to the SiC fibers and protects them from eroding by the matrix titanium alloy during the consolidating process at elevated temperature.

The average strength of fibers is the function of the Weibull modulus and reference strengths and can be expressed as[7]

$$\sigma_{avg} = \sigma_0 \Gamma(1 + \frac{1}{m}) \tag{2}$$

where  $\Gamma$  is a gamma function.

The Weibull modulus, reference strength and average strength for the three type of fibers are shown in Table 1. All of them are decreased after consolidation compared to the original fibers.

**3.2 Tensile strength of TMCs**

TMCs with different SiC fibers exhibit different tensile strengths, as shown in Fig.4. The higher tensile strength of SiC fiber corresponds to higher tensile

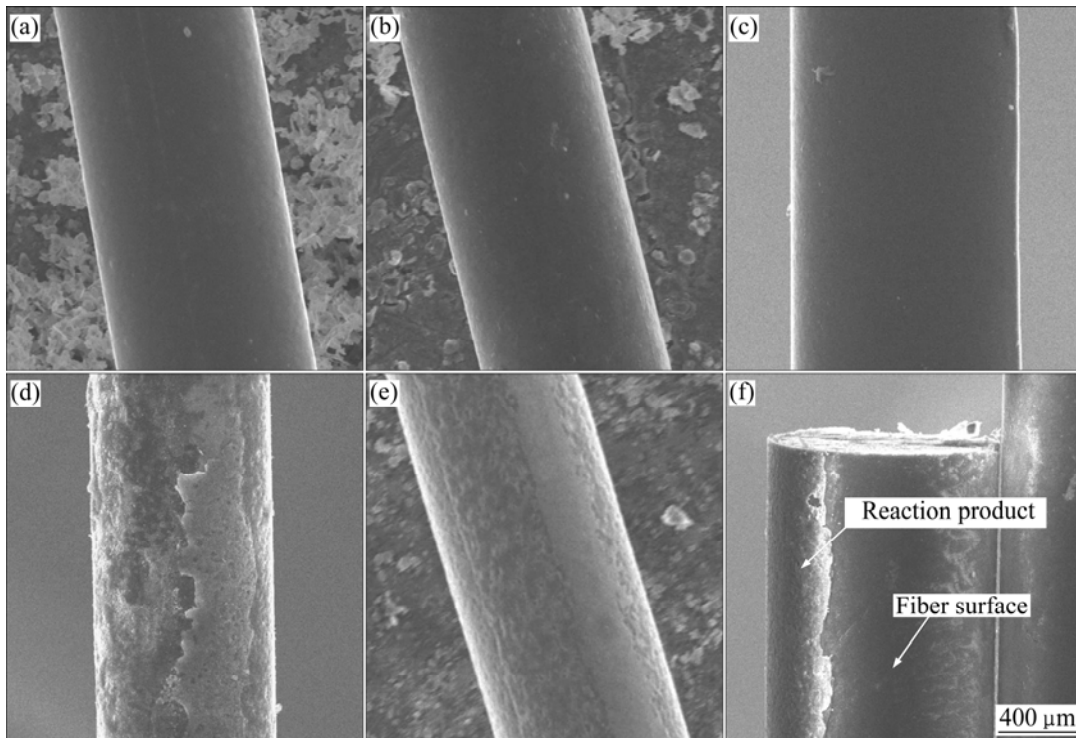
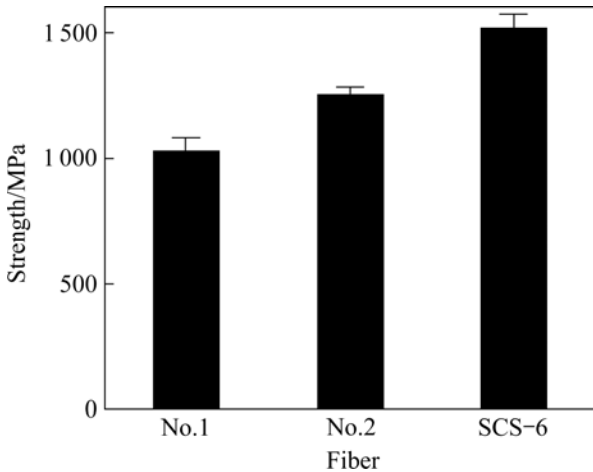


Fig.3 SEM micrographs of surfaces of pristine fibers: (a) No.1 fiber; (b) No.2 fiber; (c) SCS-6 fiber; (d) No.1 fiber extracted from TMCs; (e) No.2 fiber extracted from TMCs; (f) SCS-6 fiber extracted from TMCs

**Table 1** Weibull parameters and average strengths of fibers

Fiber	No.1			No.2			SCS-6		
	$m$	$\sigma_0/\text{MPa}$	$\sigma_{\text{avg}}/\text{MPa}$	$M$	$\sigma_0/\text{MPa}$	$\sigma_{\text{avg}}/\text{MPa}$	$m$	$\sigma_0/\text{MPa}$	$\sigma_{\text{avg}}/\text{MPa}$
Original	8.4	2 992	2 824	12.2	4 136	3 965	15.3	4 841	4 677
Extracted	3.6	2 269	2 044	6.0	2 631	2 440	9.0	3 551	3 363

**Fig.4** Tensile strength of TMCs with different fibers

strength of TMCs. The strength of the composite with SCS-6 fiber is about 500 MPa higher than that with No.1 SiC fiber.

It is crucial to take into account the residual stresses which have great effects on the mechanical properties of TMCs to evaluate the tensile strength of TMCs. The residual stresses develop in metal-matrix composites during cooling from the processing temperature, as a result of the thermal expansion mismatch between matrix and reinforcements. The following method is used to measure the residual strains in the SiC fibers. Removing the matrix with an aqueous solution of HF acid of 40%, without the restriction of metal matrix the fibers will be elongated. By measuring the variation of the length of fibers, the residual strain in SiC fibers is equal to  $-0.212\%$ . Therefore, the residual thermal stress in the SiC fiber can be determined as

$$\sigma_f^r = E_f \varepsilon_f^r = -848 \text{ MPa} \quad (3)$$

where  $E_f$  is the elastic modulus of SiC fiber, which is about 400 GPa[7–12].  $\varepsilon_f^r$  is the residual strains in the fibers.

According to the balance of residual stresses between fibers and matrix, the residual stress in the matrix titanium alloy,  $\sigma_m^r$  is calculated by a concircle model[13] and the magnitude is about 363 MPa.

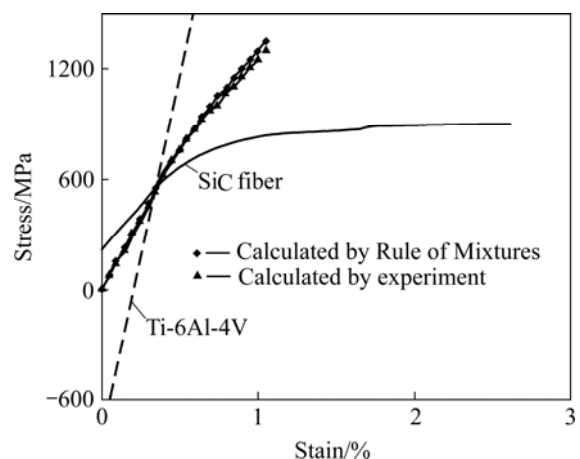
The longitudinal strength of continuous fiber reinforced titanium-matrix composites is primarily dependent on the matrix tensile properties and the fiber

strength. Taking into account the residual stress, the Rule of Mixtures for the longitudinal strength of TMCs is depicted as follows[7]:

$$\sigma_{\text{comp}}(\varepsilon) = v_f \sigma_f(\varepsilon + \varepsilon_f^r) + (1 - v_f) \sigma_m(\varepsilon + \varepsilon_m^r) \quad (4)$$

where  $v_f$  is the volume fraction of fibers,  $\sigma_{\text{comp}}(\varepsilon)$ ,  $\sigma_f(\varepsilon + \varepsilon_f^r)$  and  $\sigma_m(\varepsilon + \varepsilon_m^r)$  denote the strength at the strains of composites, SiC fiber and Ti alloy, respectively.

The stress—strain curves of single SiC fiber, TMCs and titanium alloy prepared with the same process as that of TMCs were measured, respectively. Preload of about  $-848$  and  $363$  MP were applied to the fiber and titanium alloy respectively. The stress—strain curves are shown in Fig.5. The curves of TMCs and the data calculated by the Rule of Mixtures are also shown in Fig.5. The two curves are very close to each other. This indicates that the Rule of Mixtures could predict the mechanical behavior of TMCs exactly. However, it is impossible to predict the failure strength of TMCs. The strength of fiber in TMCs is a statistical distribution, and that the broken fibers will change the stress condition of neighbor fibers. So the strength of fibers in TMCs is uncertain and the Rule of Mixtures can not be applied to calculate the fracture strength of TMCs.

**Fig.5** Stress—strain curves of experimental and calculated values

### 3.3 Interface and fractography of TMCs

The interfaces of the TMCs reinforced by No.1 fiber without carbon coating and by No.2 fiber with carbon coating are shown in Fig.6. Under the same processing

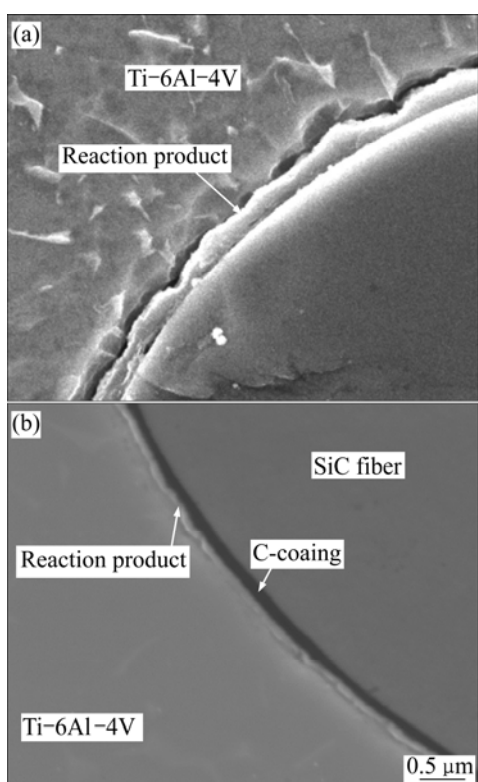


**Fig.6** SEM micrographs of interfaces of TMCs reinforced by: (a) No.1 fiber TMCs; (b) No.2 fiber with C-coating

conditions, the fiber/matrix interfacial reaction of the former is more serious than that of the latter, and there still exists some carbon coating unexhausted during the consolidation process at elevated temperature in the latter, as shown in Fig.6(b). Fig.7 shows the longitudinal section of the TMCs reinforced with SCS-6 fiber. There are also some reaction products and unexhausted C-coating in the interface. The carbon coating on the surface of SiC fiber can prevent the direct reaction between the fiber and matrix alloy, so it decreases the damage by the reaction on the surface of SiC fiber. YANG et al[17] studied the interface of  $\text{SiC}_f/\text{Ti6Al4V}$  and confirmed that the reaction products are TiC,  $\text{Ti}_3\text{Si}_3$  and  $\text{Ti}_3\text{SiC}_2$  in the interface of TMCs reinforced with uncoated SiC fibers and only TiC in the interface with carbon coating. There are different reaction mechanisms for the two types of fiber reinforced TMCs, so the reaction products of two interfaces contain different characteristic and lead to different mechanical properties of the interfaces.

The fracture surfaces of the three types of TMCs were observed by SEM. The typical fracture surfaces of the composites are shown in Fig.8. It can be found that the C-coating layers of No.2 (Fig.8(b)) and SCS-6 (Fig.8(c)) SiC fibers are debonding from the fibers seen. These imply a weak interfacial bonding. There is no distinct debonding gap observed between the matrix

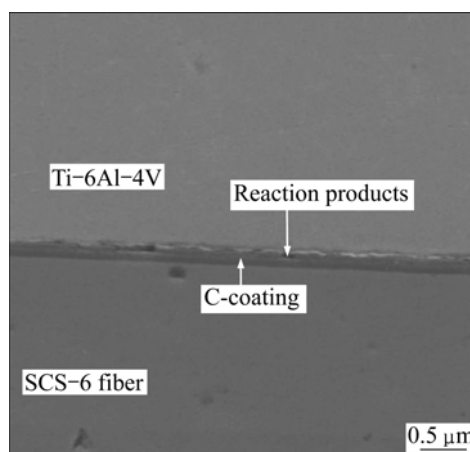


**Fig.7** Interface of SCS-6/Ti-6Al-4V

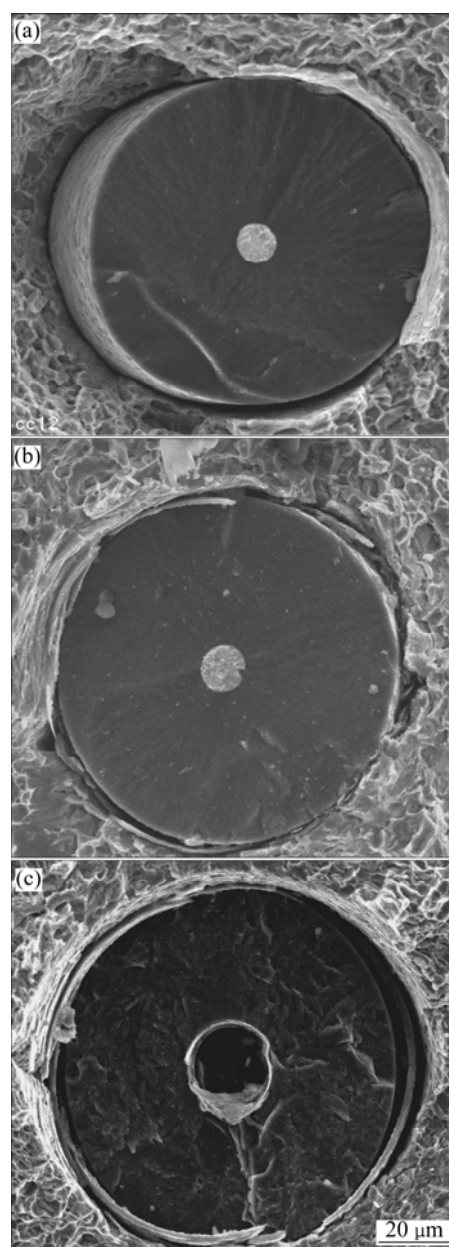


**Fig.8** Fracture surfaces of TMCs reinforced with No.1 fiber(a), No.2 fiber(b) and SCS-6 fiber(c)

and a large gap between the fiber and the matrix can be and the SiC fiber without C-coating, as shown in Fig.8(a), indicating a strong interfacial bonding. It is easy to understand that the strong interfacial bonding is due to the interfacial reaction products between the matrix Ti-6Al-4V and the SiC fiber but not the C-coating. It is also shown in Fig.8 that the fracture surfaces of No.1 and No.2 fibers are flatter than that of SCS-6 fiber, so the former two types of SiC fibers are more brittle.

### 3.4 Failure prediction for TMCs

The theoretical models for strength of TMCs generally assume that the composites fail as a consequence of the random accumulation of fiber breaking in the composites, or by the action of localized stress concentrations near the initial broken fiber, causing further fiber failure. These models are categorized as Global Load Sharing (GLS) and Local Load Sharing (LLS) models according to the condition whether local stress concentrations caused by the failure fiber are significant enough to alter the random nature of damage accumulation in TMCs.

#### 3.4.1 Critical strength and critical length of SiC fiber in TMCs

When the stress in the matrix reaches the yield stress, the matrix will not carry additional load, all the additional load must be carried by the fibers. Once the fibers begin to fail, it is assumed that the fiber-matrix interface debonds around each crack and the fibers slide with a sliding resistance relative to the matrix. The critical strength  $\sigma_c$  and critical length of fiber  $\delta_c$  in TMCs were obtained according to the relationship of the fiber strength statistics and the fiber slip in the TMCs [7, 8, 10, 11].

$$\sigma_c = \left( \frac{\sigma_0^m \tau L_0}{r} \right)^{\frac{1}{m+1}} \quad (5)$$

$$\delta_c = \left( \frac{\sigma_0 r L_0^{1/m}}{\tau} \right)^{\frac{m}{m+1}} \quad (6)$$

Referring to the experimental data [6, 7, 14],  $\tau$  is about 120 MPa for No.2 fiber and SCS-6 fiber, both with carbon coating;  $\tau$  is about 220 MPa for No.1 fiber carbon coating. According to the characteristic parameter  $\sigma_0$ ,  $L_0$  and  $m$  measured for the fibers extracted from the TMCs,

the critical strength and length for the three types of the fibers are calculated, as listed in Table 2.

#### 3.4.2 Global Load-Sharing model

The GLS model was developed to predict the strength of metal matrix composites [7]. The composites were thought of as a series of independent links, with a link length equal to twice the sliding length of the fiber in the matrix. The model adopts the following expression [8–10]:

$$\sigma_{\text{comp}} = f \sigma_c \left( \frac{2}{m+2} \right)^{\frac{1}{m+1}} \left( \frac{m+1}{m+2} \right) + (1-f) \sigma_{\text{my}} \quad (7)$$

where  $\sigma_{\text{my}}$  is the strength of matrix when the composite is broken. It is usually about 1.0%–1.3% for the longitudinal failure strain of TMCs, and the residual strain of matrix titanium alloy in TMCs is about 0.4%. Therefore, the strain of matrix is 1.4%–1.7% when the composite fails at the longitudinal load. In terms of the stress–strain curve for Ti-6Al-4V alloy, as shown in Fig.5,  $\sigma_{\text{my}}$  is about 900 MPa at the strain of 1.4%–1.7%. The calculated results of the composite are also shown in Table 2.

#### 3.4.3 Local Load-Sharing model

It is supposed in the LLS model that the strength of the composite can be influenced by many factors, including the strength distribution of the reinforcement fibers, stress concentration in neighboring fibers which in turn, depend on the fiber, matrix and interface properties. TMCs fracture is induced by the unstable propagation of a cluster formed by several broken fibers, and the composite strength can be determined by calculating the probability of nucleating clusters with 1, 2, 3 or more adjacent broken fibers [11].

Without consideration of the influence of stress concentration, at the stress  $\sigma_f$ , the fracture probability of fibers in TMCs will be

$$F(\sigma_f) = N \left\{ 1 - \exp \left[ - \frac{L}{L_0} \left( \frac{\sigma_f}{\sigma_0} \right)^m \right] \right\} \quad (8)$$

where  $L$  is the gauge length of TMCs specimen;  $N$  is the number of fibers in gage part of TMCs and it is 140 for SCS-6/Ti-6Al-4V and 220 for the composites reinforced by the other two kinds of Chinese SiC fibers.

**Table 2** Experimental and model prediction results for TMCs

Ti-6Al-4V composite reinforced by	$\sigma_c$ /MPa	$\delta_c$ /μm	$\sigma_{\text{comp}}$ /MPa				
			Experiment	GLS	LLS, $n=1$	LLS, $n=2$	LLS, $n=3$
No.1 fiber	5 176	1.29	1 036±47	1 649	*	996	1 065
No.2 fiber	4 057	1.86	1 260±26	1 503	1 046	1 166	1 224
SCS-6 fiber	4 555	2.65	1 521±52	1 677	1 276	1 454	1 496

\* The calculated strength of composite is less than the strength of matrix.

It is assumed that a single fiber failure leads to the composite failure, then  $F(\sigma_f)=1$ , Eqn.(8) will be close to

$$F_1(\sigma_f) \approx N \frac{L}{L_0} \left( \frac{\sigma_f}{\sigma_0} \right)^m = 1 \quad (9)$$

At this situation, the maximum stress that fibers can stand in the TMCs is

$$\sigma_f^{u1} = \sigma_0 \left( \frac{L_0}{NL} \right)^{1/m} \quad (10)$$

The failure probability of two neighbor fibers failure at the same time is given by

$$F_2(\sigma_f) = 1 - (1 - F)^{n_i} = 1 - \exp \left\{ \frac{-2n_i}{L_0} \left[ \frac{\sigma_f}{\sigma_0} \right]^m \int_0^{\delta_c} (1 + k_1) dz \right\} \quad (11)$$

where  $n_i$  is the number of neighbor fibers adjacent to a broken one. The fibers are arranged in a hexagonal array, so  $n_i$  is equal to 6.  $k_1$  is the stress concentration factor (SCF). Referring to Ref.[9],  $k_1$  is about 4% for No.2 and SCS-6 SiC fibers composites which contain a weak carbon structure interface, and about 10 % for No.1 fiber composite with strong interface.

Eqn.(11) can also be expressed as

$$F_2(\sigma_f) \approx \frac{C_2}{L_0} \left( \frac{\sigma_f}{\sigma_0} \right)^m \quad (12)$$

$$\text{where } C_2 = 12 \int_0^{\delta_c} (1 + k_1)^m dz$$

Assume that two neighbor failure fibers form a cluster which can induce the composite fracture. Then  $F_2(\sigma_f)=1$ , and the whole fibers strength in TMCs is

$$\sigma_f^{u2} = \sigma_0 \left( \frac{L_0^2}{NLC_2} \right)^{\frac{1}{2m}} \quad (13)$$

The same treating process is employed to calculate the whole fibers strength in TMCs to which three neighbor fibers will lead to failure.

$$\sigma_f^{u3} = \sigma_0 \left[ \frac{L_0^3}{NLC_2 C_3} \right]^{\frac{1}{3m}} \quad (14)$$

$$C_3 = 12 \int_0^{\delta_c} (1 + k_1)^m dz + 4 \int_0^{\delta_c} (1 + 2k_1)^m dz$$

It will be more complicated for 4 or more neighbor fibers failure inducing TMCs fracture.

Giving the fibers cluster strength in TMCs, the failure strength of the TMCs will be calculated by employing the Rule of Mixtures expressed as follows:

$$\sigma_{\text{comp}} = f \sigma_f^u + (1 - f) \sigma_{\text{my}} \quad (15)$$

where  $\sigma_f^u$  is the strength of fibers cluster in TMCs.

The measured strengths and the calculated ones of the three composites are shown in Table 2. The GLS model gives the overestimated strengths for all three composites, especially for the one reinforced with the No.1 fibers, about 600 MPa higher than the experimental value. This is due to that the model does not consider the effect of broken fibers on other fibers and the interfacial properties of the composites. On the contrary, in the LLS model, one-fiber failure model underestimates the strengths of the three composites, and so does the two-fiber failure model, but the prediction of the latter is closer to the experimental values. However, it can be found in Table 2 that the calculated data by the three-fiber failure of the LLS model are nearly equal to the measured values for all the three kinds of TMCs. This indicates that the failure of the TMCs is due to the unstable propagation of a cluster formed by at least three adjacent broken fibers prior to the appearance of widespread damage in the sample.

## 4 Conclusions

1) Consolidating the TMCs at high temperature degenerates the mechanical properties of the reinforcement fibers. Therefore, it is the strength of the fiber extracted from the TMCs but not that of the original fiber that should be used to calculate the strength of the TMCs.

2) The predicted strength by GLS model is higher than the measured one, although the model can get better results for the TMCs with lower interfacial bonding and with the SiC fiber having higher Weibull module. The strength predicted by the LLS model is exactly enough to the measured data when taking three-fiber failure into account. It means that three broken neighbor fibers can form a critical crack that makes the TMCs break.

## References

- [1] YANG Yan-qing, ZHU Yan, CHEN Yan. Processing and property of SiC fiber reinforced Ti-matrix composite [J]. Rare Metal Materials and Engineering, 2002, 31(3): 201–205. (in Chinese)
- [2] ZHOU Yi-gang, YANG Yan-qing. Progress in the study of titanium matrix composite reinforced by SiC fibers[J]. Acta Metallurgica Sinica, 2002, 38 (Suppl): 461–464. (in Chinese)
- [3] YANG Yan-qing, MA Zhi-jun, LI Jian-kang. CHEN yan. Interfacial reaction and its effects on mechanical property of SiC/Super  $\alpha_2$  composites [J]. Rare Metal Materials and Engineering, 2006, 35(1): 43–49. (in Chinese)
- [4] FU Yue-chun, SHI Nan-lin, ZHANG De-zhe, YANG Rue. Preparation of SiC/Ti composites by powder cloth technique [J]. The Chinese Journal of Nonferrous Metals, 2004, 14(3): 465–470. (in Chinese)
- [5] LÜ Xiang-hong, YANG Yan-qing, HUANG Bin, LUO Xian, LIU Yu-cheng. Reaction diffusion in continuous SiC fiber reinforced Ti matrix composites [J]. Trans Nonferrous Met Soc China, 2007, 17(1):

27–34.

- [6] BEDNARCYK B A, ARNOLD S M, ABOUDI J. Local field effects in titanium matrix composite subject to fiber-matrix debonding [J]. *International Journal of Plasticity*, 2004, 20: 1707–1737.
- [7] GUNDEL D B, WAWNER F E. Experimental and theoretical assessment of the longitudinal tensile strength of unidirectional SiC-fiber/titanium-matrix [J]. *Composites*, 1997, 57: 471–481.
- [8] TURON A, COSTA J, MAINI P. A progressive damage model for unidirectional fiber-reinforced composites based on fiber fragmentation [J]. *Composites and Technology*, 2005, 65: 2039–2048.
- [9] THOMAS M P, WINSTONE M R. Longitudinal yielding behavior of SiC-fiber-reinforced titanium matrix composite [J]. *Composites and Technology*, 1999, 59: 297–303.
- [10] MAJUMDAR B S, MATIKAS T E, MIRACLE D B. Experiments and analysis of fiber fragmentation in single and multiple-fiber SiC/Ti-6Al-4V metal matrix composites [J]. *Composites (Part B)*, 1998, 29: 131–147.
- [11] GONZALEZ C, LLORCA J. Micromechanical modeling of deformation and failure in Ti-6Al-4V/SiC composites [J]. *Acta Mater*, 2001, 49: 3505–3519.
- [12] FUKUSHIMA A, FUJIWARA C, KAGAWA Y. Effect of interfacial properties on tensile strength in SiC/Ti-15-3 composites [J]. *Materials Science and Engineering A*, 2000, 276: 243–249.
- [13] PICKARD S M, MICRACLE D B, MAJUMDAR B S, KENDIG K L. An experimental study of residual fiber strains in Ti-15-3 continuous fiber composites [J]. *Acta Metall Mater*, 1995, 43(8): 3105–3112.
- [14] MUKHERJEE S, ANANTH C R, CHANDRA N. Effects of interface chemistry on the fracture properties of titanium matrix composites [J]. *Composites (Part A)*, 1998, 29: 1213–1219.
- [15] RAMAMURTY U. Assessment of load transfer characteristics of a fiber-reinforced titanium matrix composite [J]. *Composites Science and Technology*, 2005, 65 (9): 1815–1827.
- [16] ARNOLD S M, PINDER M J, WILT T E. Influence of fiber architecture on the inelastic response of metal matrix composites [J]. *International Journal of Plasticity*, 1996, 12(4): 507–545.
- [17] YANG Yan-qing, MA Zhi-jun, LÜ Xiang-hong. Studies on interface of SiC<sub>f</sub>/Ti-6Al-4V composites [J]. *Rare Metal Materials and Engineering*, 2006, 35(10): 1516–1523. (in Chinese)

(Edited by YUAN Sai-qian)